



## An ultrafast one-step assay for the visual detection of RNA virus†

Cite this: DOI: 10.1039/c8cc00150b

Received 8th January 2018,  
Accepted 23rd February 2018

DOI: 10.1039/c8cc00150b

rsc.li/chemcomm

Cuiping Ma,<sup>a</sup> Hao Jing,<sup>a</sup> Pansong Zhang,<sup>a</sup> Lingzhi Han,<sup>a</sup> Meiling Zhang,<sup>a</sup>  
Fuxin Wang,<sup>a</sup> Shuyan Niu<sup>a</sup> and Chao Shi<sup>\*,b</sup>

**A one-step, rapid, and visual method was developed for the detection of RNA viruses and a few copies of the Zika RNA virus were directly detected within 25 min by naked-eye observation. This method will prove to be promising for point-of-care testing in out-of-lab and inconvenient settings.**

RNA viruses such as the Zika virus,<sup>1,2</sup> Ebola virus,<sup>3</sup> influenza virus,<sup>4</sup> and the human immunodeficiency virus (HIV)<sup>5</sup> have captured attention due to large worldwide outbreaks resulting in global health crises. Therefore, it is essential to develop a simple, rapid, and effective detection method in order to prevent and control large outbreaks of RNA viruses. Nucleic acid-based detection approaches, such as real-time PCR,<sup>6–8</sup> can often offer accurate and rapid diagnosis of RNA viruses. However, PCR and PCR-derived techniques require an additional reverse transcription step in order to transcribe RNA into the complementary DNA (cDNA) strand.<sup>9</sup> In addition, nucleic acid amplification reaction by PCR needs to be repeatedly heated and cooled. As a result, complicated operation, long reaction time, and relatively expensive equipment are required. Considering the large-scale outbreak of RNA viruses, such as Zika virus,<sup>10</sup> the development of a rapid and simple detection approach is of importance. It was previously reported that *Bst* DNA polymerase possesses innate reverse transcriptase activity.<sup>11</sup> Excitingly, this report provides a new insight for the one-step detection of RNA.<sup>12</sup> Based on this finding, strand exchange amplification method, namely, SEA was developed.<sup>13</sup> However, the SEA method shows unsatisfactory sensitivity for actual application as it utilizes the natural strand “breathing” of unwound dsDNA rather than heat denaturation.<sup>2</sup> In this study, one-step visual detection of RNA viruses with high

sensitivity was realized using the advanced strand exchange amplification (ASEA).

To realize one-step detection of RNA virus with high sensitivity, we attempted to combine the SEA method with different isothermal amplification strategies. In 2003, an exponential amplification reaction (EXPAR) was reported, which could achieve 10<sup>6</sup>–10<sup>9</sup> fold amplification in several minutes using a DNA polymerase and a nicking endonuclease.<sup>14,15</sup> The combination of SEA with EXPAR was tested to detect RNA viruses (Fig. S1 and Table S1, ESI†). A high non-specific background hindered the further development of this detection approach although EXPAR greatly increased the sensitivity of SEA (Fig. S2, ESI†).<sup>16,17</sup>

Restriction endonucleases (REases) are used as a crucial enzyme tools in biotechnological applications. Herein, the REase was combined with SEA in order to increase the sensitivity of SEA and referred to as ASEA henceforth (Fig. 1). In brief, the ASEA method employs dynamical dissociation of the DNA duplex including cleaved products by REase; the cleaved products therefore can work as primers to initiate the extension by DNA polymerase. During the reaction, REase and DNA polymerase repeatedly function together to achieve exponential amplification. Herein, RNA was taken as an example. As illustrated in Fig. 2, when the target RNA was present, primer P1 was extended with the activity of reverse transcriptase of *Bst* DNA polymerase to form a heterogeneous hybrid of DNA and RNA. The interaction of each base pair of DNA is weak, allowing it to open transiently, which results in a single-stranded denaturation bubble under the reaction temperature.<sup>13,18</sup> Primer P2 could invade the denaturation bubble and was then extended to generate the dsDNA amplification products of the two primers P1 and P2. Primer P3 was designed to contain the restriction recognition site of *Bsr* I. When Primer P3 invaded the denaturation bubble of amplification product of P1 and P2 and hybridized, the complementary strand of P3 was extended, forming the cutting site of *Bsr* I. In the presence of *Bsr* I, the extended amplification products were cleaved under reaction temperature, generating two short dsDNA fragments that were used as primers after dynamical dissociation followed by the extension with primer

<sup>a</sup> College of Marine Science and Biological Engineering, Key Laboratory of Sensor Analysis of Tumor Marker, Ministry of Education, College of Chemistry and Molecular Engineering, Qingdao University of Science and Technology, Qingdao, 266042, P. R. China

<sup>b</sup> College of Life Sciences, Qingdao University, Qingdao, 266071, P. R. China.  
E-mail: sc169@163.com

† Electronic supplementary information (ESI) available. See DOI: 10.1039/c8cc00150b

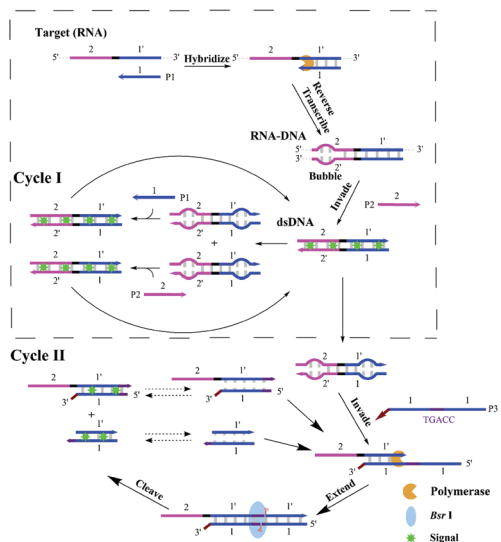


**Fig. 1** Schematic diagram of the advanced strand exchange amplification (ASEA) for detection of RNA viruses. The target was divided into different domains marked with the numbers. Numbers marked with a prime symbol (') were complementary to the corresponding unmarked number. The dotted box was for the strand exchange amplification (SEA). All sequences used herein are listed in Table S1 (ESI<sup>†</sup>).

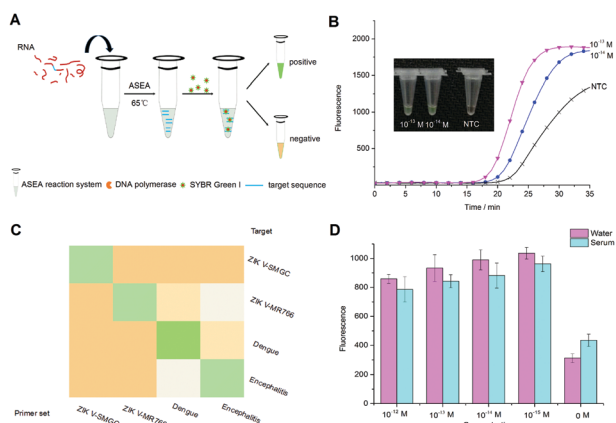


**Fig. 2** The sensitive, isothermal, and one-step biosensing for Zika virus RNA detection. (A) The schematic illustration of isothermal ASEA method to detect Zika virus RNA. (B) The real-time fluorescence curves for different concentrations of Zika virus RNA; NTC was control without target. Inset, the visual detection of Zika virus RNA. The positive was green and the negative was orange. (C) Orthogonality of primer sets of Zika virus (GenBank: KX266255, strain SMGC), Zika virus (GenBank: AY632535, strain MR766), Dengue virus (GenBank: AF326573) and Japanese Encephalitis virus (GenBank: EF623988) corresponding to  $1.0 \times 10^{-13}$  M synthetic trigger DNA from each of four virus. Green indicated maximum biosensing activation and orange indicated no biosensing activation. (D) Anti-interference of Zika virus RNA detection. Zika virus RNA was added to water or 7% human serum and was amplified by ASEA method at  $65^\circ\text{C}$  for 25 min with target concentrations ranging from  $1.0 \times 10^{-12}$  M to  $1.0 \times 10^{-15}$  M. Error bars represented standard deviation (SD) from three replicates.

P3 as templates. Thus, the dsDNA amplification products continued to be digested to generate two new short dsDNA amplification products. In summary, a rapid and exponential amplification was

realized for sensitive detection by dynamical dissociation of DNA combined with REase and DNA polymerase.

First, the feasibility of the ASEA method was investigated by detecting different concentrations of genomic DNA from *Vibrio parahaemolyticus* (*V. parahaemolyticus*) ATCC17802. The results indicated that ASEA was effective in detecting *V. parahaemolyticus* genomic DNA through fluorescence and colorimetric assays (Fig. S3, ESI<sup>†</sup>).

Considering that *Bst* DNA polymerase has been reported to possess innate reverse transcriptase activity and can be used for one-step RNA detection,<sup>11,13</sup> in this study, we examined whether ASEA would work on RNA viruses. The extracted Zika virus RNA was directly used to trigger ASEA without reverse transcription (Fig. 2A). The rapid increase in the fluorescence signal was observed when  $1.0 \times 10^{-13}$  M and  $1.0 \times 10^{-14}$  M Zika virus RNA were used as targets (Fig. 2B). A S-shaped amplification curve indicated an approximately exponential increase in oligonucleotide product yield. To fulfill the detection requirement of a low-resource setting, a visual detection method was established. A concentration of  $40 \times$  SYBR Green I was placed on the lid in advance and then mixed with the above-described reaction mixtures after the amplification reaction. The colorimetric plots are shown in Fig. 2B. The color of positive reactions ranged from orange to green, while the color of the negative reaction was still orange. The detection of different concentrations of Zika virus RNA was also investigated by the fluorescence and colorimetric methods (Fig. S4, ESI<sup>†</sup>). All chosen concentrations of the Zika virus RNA including the lowest ( $1.0 \times 10^{-15}$  M) could be well distinguished from the negative control by fluorescence. Thus, these results confirmed that the ASEA method could successfully detect the RNA virus with the advantages of one-step, isothermal amplification, and visualization.

Under optimum conditions (Fig. S5 and S6, ESI<sup>†</sup>), different concentrations of the Zika virus RNA were investigated to determine the detection limit of ASEA. The serial 10 fold dilutions of Zika virus RNA ranging from  $1.0 \times 10^{-15}$  M to  $1.0 \times 10^{-18}$  M were used to trigger ASEA reactions and incubated at  $65^\circ\text{C}$  for 25 min. The fluorescence intensities corresponding to different concentrations of RNA targets significantly increased when compared with the non-target controls (NTCs) (Fig. 3A). Therefore, every reaction containing the target molecule could be significantly distinguished from that without target. In addition, the positive and NTC were still distinguishable even when the target RNA concentration was as low as  $1.0 \times 10^{-18}$  M (about six copies in the reaction mixture). However, a good linear relationship between the fluorescence intensity and the target concentration was not observed, which is consistent with some other nucleic acid detection methods.<sup>2,19,20</sup> Thus, this is an area of confusion for many studies of isothermal nucleic acid detection. Herein, we inferred that this problem may be related to the semi-random occurrence of the denaturation bubble as well as the combination of endonuclease and polymerase. A minimum Zika virus concentration of  $1.2 \times 10^{-15}$  M in patient serum has been previously reported in the literature<sup>2</sup> and higher loading of  $3.65 \times 10^{-13}$  M,  $4.9 \times 10^{-15}$  M, and  $4.1 \times 10^{-15}$  M have been found in urine, patient saliva, and primate serum,<sup>2</sup> respectively.

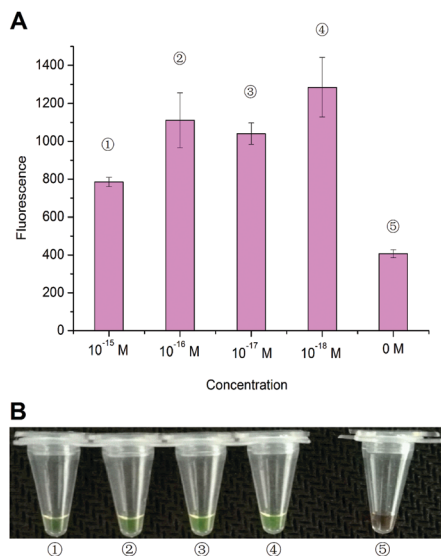


**Fig. 3** Detection limit of Zika virus. (A) Serial 10-fold dilutions of Zika virus RNA were used to trigger ASEA reaction. Error bars represented SD from three replicates. (B) Colorimetric detection for different concentrations of Zika virus RNA. The concentrations of Zika virus RNA were ①  $1.0 \times 10^{-15}$  M, ②  $1.0 \times 10^{-16}$  M, ③  $1.0 \times 10^{-17}$  M, ④  $1.0 \times 10^{-18}$  M, and ⑤ 0 M.

Accordingly, the ASEA method displayed high sensitivity for the Zika virus RNA trigger and was able to easily detect it at clinically relevant RNA concentrations.

The colorimetric results for Zika virus detection were further shown in Fig. 3B. There was a significant color change for positive samples, while no color change was observed for the negative reaction. Thus, these results demonstrated that concentrations as low as  $1.0 \times 10^{-18}$  M of Zika virus RNA could be vividly discriminated against NTC and visualized by color change.

To test the sensor specificity against viruses that share high similarity and clinical symptoms with Zika virus, we focused on the possible cross-reactivity of Zika virus sensors. Although our primer set was designed based on the Zika virus genomic sequence (GenBank: KX266255, strain SMGC) that is mostly distinct from that of related viruses, the target Zika sequences do share substantial similarity with the Dengue virus and Japanese Encephalitis virus (Fig. S7, ESI<sup>†</sup>).<sup>21</sup> To test possible cross-reactivity for the ASEA method, primer sets of the Dengue virus (GenBank: AF326573) and Japanese Encephalitis virus (GenBank: EF623988) corresponding to regions that share a degree of homology with that of target Zika genome DNA were designed. In addition, different subtypes of the Zika virus were aligned and the strain MR766 (GenBank: AY632535) was chosen as the representative of African lineage to design the corresponding primer set. All sequences used in this study are listed in Table S2 (ESI<sup>†</sup>). The annealing temperature of each primer set was optimized. The specificity for different primer sets to their targeted sequences and related non-targeted sequences were investigated and the results of fluorescence detection for sequence specificity of ASEA method are shown in Fig. S8 (ESI<sup>†</sup>). The orthogonality of primer sets to the  $1.0 \times 10^{-13}$  M synthetic target DNA from different viruses was performed to further

investigate the specificity of colorimetric detection (Fig. 2C). When the primer sets were exposed to their related non-targeted sequences, ASEA failed to be triggered and orange color was still observed. Conversely, the color change of reaction system from orange to green indicated maximum sensor activation, when the primer sets were exposed to their targeted sequences. Although the negative control was light-green due to weak specificity of primer sets of Dengue virus and Japanese Encephalitis virus, the positive samples still could be significantly distinguished from the negative controls by colorimetric detection. Thus, robust sequence specificity was demonstrated in our amplification and colorimetric detection scheme by the specific detection of related virus homology region.

To validate whether ASEA is a promising candidate for application in clinical samples, the trigger RNA was spiked into diluted human serum (7%), heated to 95 °C for 2 min, followed by triggering the ASEA reaction at 65 °C for 25 min. The fluorescence intensity of the human serum sample was observed to be nearly the same as that of water, both of which could be significantly distinguished from their negative controls (Fig. 2D). The detection of Zika virus RNA was proved to be reliable for samples spiked into low concentration of serum. Therefore, the results indicated that the ASEA method exhibited strong anti-interference ability for its utilization in real clinical samples.

In conclusion, the detection of RNA viruses is a critical issue for monitoring the rapid proliferation of viral infections.<sup>22,23</sup> Although traditional RNA detection methods have been widely developed, rapid diagnosis is often limited due to long durations and the additional step of reverse transcription.<sup>2,12</sup> Based on our previous finding that *Bst* DNA polymerase has innate reverse transcriptase activity, a one-step, rapid, and sensitive nucleic acid isothermal amplification method was successfully developed by combining the dynamical dissociation of DNA with the interaction between restriction endonucleases and DNA polymerase, which is a promising response to any emerging virus outbreak. The simplicity of RNA reverse transcription and amplification in a single step is desirable to achieve point-of-care testing (POCT) applications and will contribute to realize the sample-to-answer process. This method was capable to directly detect a few copies of Zika virus RNA in the reaction system within 25 min. Thus, the ASEA method is promising with clinically relevant sensitivity for low abundance of nucleic acid targets in most of clinical samples and the small samples used in POCT. In addition, this method only required a pair of primers, which was more suitable to detect target sequences with high mutation rates as compared to loop-mediated isothermal amplification (LAMP) that required four primers and six specific target domains.<sup>12</sup> In order to enable our method to be employed in remote areas and inconvenient situations, a visual colorimetric detection method was developed and the output could be observed by the naked eye. Moreover, our method may be compatible with other signal outputs, such as molecular beacon and toehold strand displacement<sup>24</sup> via small change of primers. Nevertheless, the visual colorimetric detection will greatly benefit POCT and provide a new way to monitor the outbreak and spread of RNA viruses, particularly when combined with microfluidic chip method.

We would like to express our thanks to Prof. Yuhai Bi for providing extracted Zika virus RNA. This study was financially supported by grants from the National Natural Science Foundation of China (31670868, 21675094) and the Shandong Province Natural Science Fund Major Basic Research Project (ZR2017ZC0123).

## Conflicts of interest

There are no conflicts to declare.

## Notes and references

- J. S. Gootenberg, O. O. Abudayyeh, J. W. Lee, P. Essletzbichler, A. J. Dy, J. Joung, V. Verdine, N. Donghia, N. M. Daringer and C. A. Freije, *Science*, 2017, eaam9321.
- K. Pardee, A. A. Green, M. K. Takahashi, D. Braff, G. Lambert, J. W. Lee, T. Ferrante, D. Ma, N. Donghia and M. Fan, *Cell*, 2016, **165**, 1255–1266.
- S. K. Gire, A. Goba, K. G. Andersen, R. S. G. Sealfon, D. J. Park, L. Kanneh, S. Jalloh, M. Momoh, M. Fullah and G. Dudas, *Science*, 2014, **345**, 1369–1372.
- N. L. Yozwiak, S. F. Schaffner and P. C. Sabeti, *Nature*, 2015, **518**, 477.
- C. Conrad, H. M. Bradley, D. Broz, S. Buddha, E. L. Chapman, R. R. Galang, D. Hillman, J. Hon, K. W. Hoover and M. R. Patel, *MMWR Morb Mortal Wkly Rep.*, 2015, **64**, 443–444.
- P. Liang and A. B. Pardee, *Science*, 1992, **257**, 967–971.
- N. R. Beer, E. K. Wheeler, L. Lee-Houghton, N. Watkins, S. Nasarabadi, N. Hebert, P. Leung, D. W. Arnold, C. G. Bailey and B. W. Colston, *Anal. Chem.*, 2008, **80**, 1854–1858.
- A. Kaushik, S. Tiwari, R. D. Jayant, A. Marty and M. Nair, *Biosens. Bioelectron.*, 2016, **75**, 254–272.
- M. W. Schmitt, E. J. Fox, M. J. Prindle, K. S. Reid-Bayliss, L. D. True, J. P. Radich and L. A. Loeb, *Nat. Methods*, 2015, **12**, 423–425.
- E. L. Hatcher, S. A. Zhdanov, Y. Bao, O. Blinkova, E. P. Nawrocki, Y. Ostapchuck and J. R. Brister, *Nucleic Acids Res.*, 2016, **45**, D482–D490.
- C. Shi, X. Shen, S. Niu and C. Ma, *J. Am. Chem. Soc.*, 2015, **137**, 13804–13806.
- N. Chotiwan, C. D. Brewster, T. Magalhaes, J. Weger-Lucarelli, N. K. Duggal, C. Rückert, C. Nguyen, S. M. G. Luna, J. R. Auver and B. Andre, *Sci. Transl. Med.*, 2017, **9**, eaag0538.
- C. Shi, F. Shang, M. Zhou, P. Zhang, Y. Wang and C. Ma, *Chem. Commun.*, 2016, **52**, 11551–11554.
- J. Van Ness, L. K. Van Ness and D. J. P. Galas, *Proc. Natl. Acad. Sci. U. S. A.*, 2003, **100**, 4504–4509.
- H. Jia, Z. Li, C. Liu and Y. Cheng, *Angew. Chem., Int. Ed.*, 2010, **49**, 5498–5501.
- X. Liang, K. Jensen and M. D. Frank-Kamenetskii, *Biochemistry*, 2004, **43**, 13459–13466.
- E. Tan, B. Erwin, S. Dames, T. Ferguson, M. Buechel, B. Irvine, K. Voelkerding and A. Niemz, *Biochemistry*, 2008, **47**, 9987–9999.
- G. Altan-Bonnet, A. Libchaber and O. Krichevsky, *Phys. Rev. Lett.*, 2003, **90**, 138101.
- Y. Ma, X. Dai, T. Hong, G. B. Munk and M. Libera, *Analyst*, 2017, **142**, 147–155.
- Y. Wang, Y. Wang, L. Zhang, D. Liu, L. Luo, H. Li, X. Cao, K. Liu, J. Xu and C. Ye, *Front. Microbiol.*, 2016, **7**, 753.
- M. W. Gaunt, A. A. Sall, X. de Lamballerie, A. K. L. Falconar, T. L. Dzhivanian and E. A. Gould, *J. Gen. Virol.*, 2001, **82**, 1867–1876.
- S. Bhadra, Y. S. Jiang, M. R. Kumar, R. F. Johnson, L. E. Hensley and A. D. Ellington, *PLoS One*, 2015, **10**, e0123126.
- Y. Du, R. A. Hughes, S. Bhadra, Y. S. Jiang, A. D. Ellington and B. Li, *Sci. Rep.*, 2015, **5**, 11039.
- Y. S. Jiang, S. Bhadra, B. Li, Y. R. Wu, J. N. Milligan and A. D. Ellington, *Anal. Chem.*, 2015, **87**, 3314–3320.